Gas and aerosol carbon in California: comparison of measurements and model predictions in Pasadena and Bakersfield

K.R. Baker[1], A.G. Carlton[2], T.E. Kleindienst[3], J.H. Offenberg[3], M.R. Beaver[3], D. R. Gentner[4], A. H. Goldstein[5], P. L. Hayes[6], J. L. Jimenez[7], J. B. Gilman[8], J. A. de Gouw[8], M. C. Woody[3], H.O.T. Pye[3], J.T. Kelly[1], M. Lewandowski[3], M. Jaoui[9], P.S. Stevens[10], W.H. Brune[11],Y.-H. Lin[12], C.L. Rubitschun[12], J. D. Surratt[12]

[1](Office of Air Quality Planning and Standards, U.S. Environmental Protection Agency, Research Triangle Park, NC)

[2](Dept. of Environmental Sciences, Rutgers University, New Brunswick, NJ)

[3](Office of Research and Development, U.S. Environmental Protection Agency, Research Triangle Park, NC)

[4](Department of Chemical and Environmental Engineering, Yale University, New Haven, CT)

[5](Department of Civil and Environmental Engineering, University of California, Berkeley, CA)

[6](Département de Chimie, Université de Montréal, Montréal, Québec, Canada)

[7](Department of Chemistry & Biochemistry, and CIRES, University of Colorado, Boulder, Colorado)

[8](Chemical Sciences Division, Earth System Research Laboratory, National Oceanic and Atmospheric Administration, Boulder, CO)

[9](Alion Science and Technology, Inc., Research Triangle Park, NC)

[10](Center for Research in Environmental Science, School of Public and Environmental Affairs and Department of Chemistry, Indiana University, Bloomington, IN)

[11](Department of Meteorology, Pennsylvania State University, University Park, PA)

[12](Department of Environmental Sciences and Engineering, Gillings School of Global Public Health, University of North Carolina at Chapel Hill, Chapel Hill, NC)

Correspondence to: K.R. Baker (baker.kirk@epa.gov)

ABSTRACT

Co-located measurements of fine particulate matter ($PM_{2.5}$) organic carbon, elemental carbon, radiocarbon (^{14}C), speciated volatile organic compounds (VOCs), and OH radical during the CalNex field campaign provide a unique opportunity to evaluate the Community Multiscale Air Quality (CMAQ) model's representation of organic species from VOCs to particles. Episode averaged daily 23-hr average ^{14}C analysis indicate $PM_{2.5}$ carbon at Pasadena and Bakersfield during the CalNex field campaign were evenly split between contemporary and fossil origin. CMAQ predicts a higher contemporary carbon fraction than indicated by the ^{14}C analysis at both locations. The model underestimates measured $PM_{2.5}$ organic carbon at both sites with very little (7% in Pasadena) of the modeled mass represented by secondary production, which contrasts with the ambient based SOC/OC fraction of 63% at Pasadena.

Measurements and predictions of gas-phase anthropogenic species, such as toluene and xylenes, are generally within a factor of 2, but the corresponding secondary organic carbon (SOC) tracer (2,3-dihydroxy-4-oxo-pentanioc acid) is systematically underpredicted by more than a factor of 2.

Monoterpene VOCs and SOCs are underestimated at both sites. Isoprene is underestimated at Pasadena and over predicted at Bakersfield and isoprene SOC mass is underestimated at both sites. Systematic model underestimates in SOC mass coupled with reasonable skill (typically within a factor of 2) in predicting hydroxyl radical and VOC gas phase precursors suggests error(s) in the parameterization of semi-volatile gases to form SOC. Yield values (α) applied to semi-volatile partitioning species were increased by a factor of 4 in CMAQ for a sensitivity simulation, taking in account recent findings of underestimated yields in chamber experiments due to gas wall losses. This sensitivity resulted in improved model performance for $PM_{2.5}$ organic carbon at both field study locations and at routine monitor network sites in California. Modeled percent secondary contribution (22% at Pasadena) becomes closer to ambient based estimates but still contains a higher primary fraction than observed.

1 INTRODUCTION

Secondary organic aerosol (SOA) forms in the atmosphere during the gas-phase photooxidation of volatile organic compounds (VOCs) that produce semi-volatile and water-soluble gases that condense to form new particles or partition to pre-existing aerosol mass (Ervens et al., 2011). SOA contributes to the atmospheric fine particulate matter ($PM_{2.5}$) burden, with subsequent effects on air quality, visibility, and climate (Hallquist et al., 2009). Despite its importance and abundance, ambient SOA mass is not well characterized by atmospheric models (Wagstrom et al., 2014). For example, the Community Multiscale Air Quality (CMAQ) model consistently underpredicts surface SOA mass concentrations for a variety of seasons and locations when compared to ambient observational estimates (Carlton and Baker, 2011;Carlton et al., 2010;Hayes et al., 2014;Zhang et al., 2014a).

SOA formation and the preceding gas-phase photooxidation chemistry are complex and often involve multiple oxidation steps in the gas, aqueous, and particle phase as well as accretion reactions in the particle phase that yield high molecular weight (MW) products. However, three-dimensional photochemical models must represent the gas-phase chemistry and SOA formation in a simplified fashion for computational efficiency (Barsanti et al., 2013). Gas-phase chemical mechanisms employ "lumped" VOC species, categorized primarily according to reactivity (e.g., reaction rate constants with the OH radical) (Carter, 2000;Yarwood et al., 2005), not product volatility or solubility. Condensable SOA-forming oxidation products are typically represented with 2 products in the standard versions of publically available and routinely applied photochemical modeling systems such as GEOS-CHEM (Chung and Seinfeld, 2002;Henze and Seinfeld, 2006) and WRF-CHEM (Grell et al., 2005) and those employed in regulatory applications for rulemaking such as CMAQ (Carlton et al., 2010) and the Comprehensive Air Quality Model with extensions (CAMx) (ENVIRON, 2014). Given the relationships between precursor VOC, OH radical abundance and SOA formation, it is important to simultaneously evaluate the model representation of all three within the context of how organic species evolve in the atmosphere to diagnose persistent SOA model bias.

Recent studies have shown that warm season SOA mass concentrations are usually greater than primary organic aerosol (POA) mass in the Los Angeles (Docherty et al., 2008;Hersey et al., 2011;Hayes et al., 2013) and Bakersfield (Liu et al., 2012) areas. Gas-to-particle condensation of VOC oxidation products dominate formation of summer SOA in Bakersfield (Liu et al., 2012;Zhao et al., 2013) and up to a third of nighttime organic aerosols (OA) in Bakersfield are organic nitrates (Rollins et al., 2012). Sources of warm season OA in Bakersfield include fossil fuel combustion, vegetative detritus, petroleum operations, biogenic emissions, and cooking (Liu et al., 2012;Zhao et al., 2013). Despite numerous studies based on observations and models, less consensus exists regarding the largest sources of warm season SOA at Pasadena. Bahreini et al. (2012) concluded that SOA at Pasadena is largely derived from gasoline engines with minimal biogenic and diesel fuel contribution (Bahreini et al., 2012). Others concluded large contributions from gasoline fuel combustion to SOA but also found notable contributions from diesel fuel combustion, cooking, and other sources (Gentner et al., 2012;Hayes et al., 2013). Zotter at al. (2014) conclude that 70% of the SOA in the urban plume in Pasadena is due to fossil sources, and that at least 25% of the non-fossil carbon is due to cooking sources. Lower volatility VOC measurements made at Pasadena have been estimated to produce approximately 30% of fresh SOA in the afternoon with a large contribution to these low volatility VOC from petroleum sources other than on-road vehicles (Zhao et al., 2014).

Chemical measurements of $PM_{2.5}$ carbon, fossil and contemporary aerosol carbon fraction, OC and its components, SOC tracers and speciated VOCs taken as part of the 2010 California Research at the Nexus of Air Quality and Climate Change (CalNex) field study in central and southern California (Ryerson et al., 2013) provide a unique opportunity to quantitatively evaluate modeled organic predictions. These special study data combined with routine $PM_{2.5}$ OC measurements in California are compared with model estimates to gauge how well the modeling system captures the gas and aerosol carbon burden using the standard CMAQ aerosol approach. The SOC mechanism in the base version of CMAQ lends itself well to comparison with chemical tracers because it retains chemical identity traceable to the precursor VOC (Carlton et al., 2010). Finally, a CMAQ sensitivity simulation was performed where the yields of semi-volatile gases from VOC oxidation were increased by a factor of 4 (Zhang et al., 2014b) to determine whether this may ameliorate the model underprediction of secondary organic carbon (SOC) seen here and in other studies (Ensberg et al., 2014).

2 METHODS

Predictions of speciated VOC, speciated COC, and aerosol-phase carbon are simultaneously compared to co-located ambient measurements at two surface locations, one in Los Angeles County (Pasadena) and one in the San Joaquin Valley (Bakersfield) air basin. The CMAQ photochemical model is applied with a fine grid resolution (4 km sized grid cells) using emissions from the 2011 National Emissions Inventory and 2010 specific point source information where available.

2.1 Model Background

CMAQ version 5.0.2 (www.cmaq-model.org) was applied to estimate air quality in California from May 5 to July 1, 2010, coincident with the CalNex Study. Gas-phase chemistry is simulated with the SAPRC07TB condensed mechanism (Hutzell et al., 2012) and aqueous-phase chemistry that oxidizes sulfur, methylglyoxal, and glyoxal (Carlton et al., 2008;Sarwar et al., 2013). The AERO6 aerosol chemistry module includes ISORROPIAII (Fountoukis and Nenes, 2007) inorganic chemistry and partitioning. The modeling system generally does well capturing ambient inorganic gases and $PM_{2.5}$ species during this time period at Pasadena and Bakersfield (Kelly et al., 2014;Markovic et al., 2014).

Model predicted OC species are shown in Figure 1 by volatility bin (log of C*) and O:C ratio (see Supporting Information for related details). Aqueous-phase species are shown with blue circles, species largely fossil in origin are colored brown and those non-fossil in origin are green. A general trend of increasing O:C ratio as volatility decreases is consistent with laboratory and field measurements (Jimenez et al., 2009). The placement of the MGLY gem-diol vertically above gas-phase MGLY in Figure 1 represents hydration processes. Aqueous-phase organic chemistry represents multiple processes, including functionalization and oligomerization, because some photooxidation products are small carboxylic acids and others are high molecular weight species (Tan et al., 2010;Carlton et al., 2007).

VOC precursors for SOA include isoprene, monoterpenes, sesquiterpenes, xylenes, toluene, benzene, alkanes, glyoxal, and methylglyoxal (Figure 1 right panel). Benzene, toluene, and xylene form SOA precursors with high-NO_X (RO_2+NO) and low-NO_X (RO_2+HO_2) specific yields (Carlton et al., 2010). CMAQ converts these precursors into multiple semi-volatile products (Figure 1 middle panel) after a single oxidation step. These multiple products vary in terms of assigned volatility and oxygen-to-carbon (O:C) ratio. When semi-volatile SOA mass oligomerizes in CMAQ the SOA identity is lost and becomes classified only as anthropogenic or biogenic, dependent on the VOC precursor (see Figure S2). After oligomerization, the saturation vapor pressure (C*) and OM:OC ratio associated with all of the 2-product semi-volatile SOA species change from the individual values to the values assigned for non-volatile, non-partitioning SOA mass (C*≈0; OM:OC = 2.1) (Carlton et al., 2010).

CMAQ VOCs and SOC species are paired in time and space with measurements (Table S2). Modeled predictions are averaged temporally to match observations and extracted from the grid cell where the monitor is located. Modeled toluene and xylene SOC are aggregated to match the measured SOC tracer (2,3-dihydroxy-4-oxopentanoic acid) which is known to represent products from both compounds and potentially other methylated aromatics (Kleindienst et al., 2004). Because the original VOCs contributing to oligomerized species are not tracked by CMAQ, biogenic oligomerized species mass is apportioned to parent VOC based on the fraction each semi-volatile SOC species contributes to the total semi-volatile (non-oligomerized) biogenic SOC at that time and location. The same technique is applied to anthropogenic SOC.

2.2 Model Application

The model domain covers the State of California and part of northwest Mexico using 4 km square sized grid cells (Figure S1). The vertical domain extends to 50 mb using 34 layers (layer 1 top ~35 m) with most resolution in the boundary layer. Initial and boundary conditions are from a coarser CMAQ simulation that used 3-hourly boundary inflow from a GEOS-Chem (v8-03-02) global model (http://acmg.seas.harvard.edu/geos/) simulation for the same period (Henderson et al., 2014). The coarser continental U.S. CMAQ simulation was run continuously from December 2009 through this study period and the first week of the finer 4 km CMAQ simulation was not used to minimize the influence of initial chemical conditions. Gridded meteorological variables are generated using the Weather Research and Forecasting model (WRF), Advanced Research WRF core (ARW) version 3.1 (Skamarock et al., 2008). Surface meteorology including temperature, wind speed, and wind direction and daytime mixing layer height were well characterized by WRF in central and southern California during this period (Baker et al., 2013).

Emissions are processed to hourly gridded input for CMAQ with the Sparse Matrix Operator Kernel Emissions (SMOKE) modeling system (http://www.cmascenter.org/smoke/). Solar radiation and temperature estimated by the WRF model are used as input to the Biogenic Emission Inventory System (BEIS) v3.14 to generate hourly emissions estimates of biogenic speciated VOC and NO (Carlton and Baker, 2011). Continuous emissions monitor (CEM) data are used in the modeling to reflect 2010 emissions information for electrical generating units and other point sources that provide that information. Day specific fires are represented but minimally impacted air quality during this period (Hayes et al., 2013). Mobile source emissions were generated using the SMOKE-MOVES integration approach (United States Environmental Protection Agency, 2014) and then interpolated between totals provided by the California Air Resources Board for 2007 and 2011. Other anthropogenic emissions are based on the 2011 National Emissions Inventory (NEI) version 1 (United States Environmental Protection Agency, 2014). Primary mass associated with carbon (non-carbon organic mass, NCOM) is estimated based on sector specific organic matter-to-organic carbon (OM:OC) ratios (Simon and Bhave, 2012).

Emissions of primarily emitted $PM_{2.5}$ OC and the sum of anthropogenic SOA precursors benzene, toluene, and xylenes (BTX) are shown in Table 1 by source sector and area. Here, the southern San Joaquin valley includes emissions from Kern, Tulare, Kings, and Fresno counties and the Los Angeles area include emissions from Los Angeles and Orange counties. BTX emissions in both areas are dominated by mobile sources (onroad and offroad) and area sources such as solvent utilization and waste disposal (Table S1). Primary OC emissions are largely commercial cooking (non-point area) in both locations with notable contribution from various types of stationary point and mobile sources. BTX emissions are almost completely fossil in origin and primarily emitted OC is split fairly evenly between contemporary and fossil origin in these areas based on the 2011 version 1 NEI (Table 1).

2.3 Sampling and Analysis Methods

CalNex ground-based measurements took place in Pasadena, CA, from 15 May – 15 June 2010 and in Bakersfield, CA, from 15 May – 30 June 2010. The Bakersfield sampling site was located in a transition area of southeast Bakersfield between the city center and areas of agricultural activity. The Pasadena sampling site was located on the California Institute of Technology campus with the Los Angeles metropolitan area to the southwest and San Gabriel Mountains directly north (see Figures S3).

An ambient-based approach is used here to estimate secondary OC from individual or groups of similar hydrocarbons (Kleindienst et al., 2010). Concentrations of specific compounds, tracers, are determined and used to estimate SOC contributions from the particular source groups based on measured laboratory tracer-to-SOC mass fractions (Kleindienst et al., 2007). Filter-based particulate matter sampling conducted at each site for 23-h periods starting at midnight (PDT) of the designated sampling day was used for tracer-based organic aerosol characterization. In total, there were 32 filter samples from Pasadena and 36 from the Bakersfield site (Lewandowski et al., 2013). The filter sampling protocols have been described in detail elsewhere (Kleindienst et al., 2010). For the analysis of the SOC tracer compounds, filters and field blanks were treated using the derivatization method described by Kleindienst et al. (Kleindienst et al., 2007). The mass spectral analysis for the organic compounds used as secondary molecular tracers has been described (Edney et al., 2003). The method detection limit (MDL) for the SOC tracer species is 0.1 ng m^{-3}. Additional details of this methodology are provided in the Supporting Information.

OC and elemental carbon (EC) concentrations were determined using the thermal-optical transmittance (TOT) method (Birch and Cary, 1996) from 1.54 cm^2 punches of quartz filters collected concurrent with the filters used for tracer analyses (hereafter referred to as UNC/EPA OC). The outer non-loaded rings were removed from filter samples then sent to Woods Hole Oceanographic Institute Accelerator Mass Spectrometry for ^{14}C analysis. The fraction of modern carbon is provided for each daily total $PM_{2.5}$ carbon sample (Geron, 2009). The modern carbon fraction is expressed as a percentage of an oxalic acid standard material that represents the carbon isotopic ratio for wood growth during 1890 (Stuiver, 1983). To account for the atmospheric ^{14}C enhancement due to nuclear bomb testing in the 1950s and 1960s, a factor of 1.044 (Zotter et al., 2014) was used to calculate the contemporary carbon fraction from the measured modern carbon result (Lewis et al., 2004;Zotter et al., 2014).

Two VOC datasets (one canister based, and one *in situ*) from each site were used in this analysis. Three hour integrated (06:00 – 09:00 PDT) canister samples for VOC analysis were collected at both sites. A total of 41 samples were collected at the Bakersfield site and 31 at Pasadena. The offline VOC analysis details are given in the Supporting Information. In Bakersfield, online VOC mixing ratios were collected for 30 minutes on the hour and analyzed via gas chromatography-flame ionization detector (GC-FID) and gas chromatography-mass spectrometry (GC-MS) (Gentner et al., 2012). In Pasadena, online VOC measurements were collected for 5 minutes every 30 minutes and analyzed via GC-MS (Borbon et al., 2013;Gilman et al., 2010). Carbon monoxide measurements at Pasadena were determined using UV fluorescence (Gerbig et al., 1999).

Hydroxyl (OH) and hydroperoxyl (HO_2) radical measurements were made at both locations using Fluorescence Assay with Gas Expansion (FAGE). The Bakersfield OH measurements used in this analysis were collected using the OH_{chem} method from the Penn State ground-based FAGE instrument (Mao et al., 2012). The Pasadena hydroperoxyl observations were made using the Indiana University FAGE instrument (Dusanter et al., 2009). HO_2 measurements from both instruments could contain an interference from various RO_2, therefore when comparing the model output with the observations, the sum of modeled HO_2 and RO_2 has been used (Griffith et al., 2013).

OC measurements from nearby Chemical Speciation Network (CSN) sites in Pasadena and Bakersfield were also used for comparison purposes. The Los Angeles CSN site (60371103) was approximately 9 miles from the CalNex site, and the Bakersfield CSN site (60290014) was approximately 3 miles from the CalNex site (see Figures S3a and S3b in the supporting information). The CSN network uses quartz-fiber filters and analyzes the carbon off-line using the thermal-optical reflectance method. Aerodyne High-Resolution Time-of-Flight Aerosol Mass Spectrometer (AMS) measurements of PM_1 OC made at Pasadena are described in Hayes et al., 2013 and online Sunset $PM_{2.5}$ OC measurements made at Bakersfield are described in Liu et al., 2012.

3 Results & Discussion

The results and discussion are organized such that the contemporary and fossil components of $PM_{2.5}$ carbon at the Pasadena and Bakersfield sites are discussed, followed by model performance for $PM_{2.5}$ carbon, speciated VOC, and SOC tracer groups. Table 2 shows episode aggregated model performance metrics for $PM_{2.5}$ organic and elemental carbon, SOC tracers, total VOC, and select VOC species. The results of a sensitivity increasing semi-volatile yields are presented throughout and discussed in detail before finally providing an evaluation of $PM_{2.5}$ carbon at all routine monitor sites in California.

3.1 Contemporary and Fossil Origins of $PM_{2.5}$ Carbon

Field campaign average total $PM_{2.5}$ carbon measurements indicate nearly equal amounts of contemporary and fossil contribution at Pasadena and Bakersfield. The field study average contemporary fraction of 23-hr average $PM_{2.5}$ total carbon samples is 0.51 at Bakersfield (N=35) and 0.48 at Pasadena (N=25). The estimate for contemporary carbon fraction at Pasadena is consistent with other ^{14}C measurements at this location for this period (Zotter et al., 2014) and similar to measurements made at urban areas in the Southeast United States: Birmingham 52% and Atlanta 63% contemporary carbon (Kleindienst et al., 2010).

Figure 2 shows observed daily 23-hr PM2.5 OC shaded by contemporary and fossil component and also PM2.5 elemental carbon. The fractional contribution of contemporary carbon to total $PM_{2.5}$ carbon is variable from day-to-day at the Pasadena site and steadily increases through the study period at the Bakersfield location (first week average of 0.44 and final week average of 0.58). Some of the contemporary carbon fraction measurements from Pasadena were above 1.0. These samples were considered erroneous and not included in the analysis and suggest the possibility of positive biases due to nearby sources (e.g. medical incinerator) in the area. It is possible some of the stronger day-to-day variability in contemporary carbon fraction measurements at Pasadena may be related to biases due to nearby “hot” sources. Higher time resolution ^{14}C measurements at Pasadena show an increase in fossil fraction during the middle of the day related to increased emissions of fossil $PM_{2.5}$ carbon precursors and SOA formation in the Los Angeles area (Zotter et al., 2014). $PM_{2.5}$ OC of fossil origin at Pasadena shows the strongest relationship to daily average temperature (Figure S4a) compared with contemporary carbon, total carbon, and elemental carbon. At Bakersfield the relationship between daily average temperature and fossil and contemporary carbon is similar (Figure S4b) and not as strong as the relationship in Pasadena. Neither fossil nor contemporary carbon concentrations show discernible patterns by day of the week at either location (Figure S5).

Modeled contemporary $PM_{2.5}$ carbon is estimated by summing primarily emitted $PM_{2.5}$ multiplied by the contemporary fraction of urban area emissions (see Section 2.1 and Table 1) with model estimated biogenic SOC species. The average baseline modeled contemporary fraction of PM2.5 OC in Pasadena is 0.51 and Bakersfield 0.54, both of which are similar to average observation estimates. However, the model shows little day to day variability in contemporary carbon fraction which does not match observed trends (Figure S6). Episode average modeled estimates of PM2.5 OC contemporary fraction are similar to the estimated contemporary fraction of the urban emissions of primary PM2.5 OC (Bakersfield=.53 and Pasadena=.51), as noted in Table 1.

3.2 $PM_{2.5}$ Carbon

Figure 3 shows measured (UNC/EPA data) and modeled $PM_{2.5}$ OC at Bakersfield and Pasadena. Organic carbon measurements from co-located instruments (AMS at Pasadena measured PM_1 and Sunset at Bakersfield measured $PM_{2.5}$) and a nearest CSN monitor are also shown in Figure 3. The co-located AMS measurements compare well with the UNC/EPA $PM_{2.5}$ organic carbon measurements at Pasadena, while the concentrations measured at the nearby CSN site are substantially lower. At Bakersfield, UNC/EPA measurements are higher compared with the nearby CSN (episode average ~3 times higher) and co-located daily average Sunset (episode average 20% higher) measured $PM_{2.5}$ OC illustrate possible measurement artifacts in the CalNex measurements at this location. These differences in measured concentration at Bakersfield may be related to filter handling, variability in collected blanks, true differences in the OC concentrations since the CSN site is spatially distinct, differences in the height of measurement (these CSN monitors are situated on top of buildings), and differences in analytical methods since CSN sites use thermal optical reflectance (TOR) to operationally define OC and EC.

Modeled $PM_{2.5}$ OC is underestimated at both CalNex locations (Figure 3), most notably at Bakersfield. However, given the large differences in $PM_{2.5}$ OC mass compared to co-located and nearby routine measurements, it is not clear which measurement best represents ambient $PM_{2.5}$ OC concentrations and would be most appropriate for comparison with the model. The model generally compares well to the CSN site nearest Pasadena and Bakersfield. $PM_{2.5}$ elemental carbon is well characterized by the model at Bakersfield (fractional bias = -13% and fractional error = 35%) and over-estimated at Pasadena (fractional bias and error = 125%) (Figure S7). Since the emissions are based on TOR and UNC/EPA measurements use the TOT operational definition of total carbon some of the model overestimation may be related to the TOR method estimating higher elemental carbon fraction of total carbon (Chow et al., 2001).

$PM_{2.5}$ OC is mostly primary (Pasadena 93% and Bakersfield 88%) in the baseline model simulation. AMS measurements at Pasadena suggest OC is mostly secondary in nature with an average of 63% for the SVOOA and OOA components for this field study (Hayes et al., 2013). Model estimated $PM_{2.5}$ OC is largely from primarily emitted sources and contemporary in nature based on the contemporary/fossil split of primary $PM_{2.5}$ emissions near both sites (Figure S6). Primarily emitted $PM_{2.5}$ OC emissions sources near Pasadena and Bakersfield include mobile sources, cooking, and dust based on emissions inventory information (Table 1). Some of these sources of primarily emitted $PM_{2.5}$ OC may be semi-volatile in nature. Model treatment of POA as semi-volatile may improve the primary-secondary comparison with observations but would likely exacerbate underpredictions of $PM_{2.5}$ OC unless oxidation and re-partitioning of the products is considered (Robinson et al., 2007). The underestimation of SOC may result from underestimated precursor VOC, poorly characterized oxidants, underestimated semi-volatile yields, missing intermediate volatility VOC emissions (Stroud et al., 2014;Zhao et al., 2014), other issues, or some combination of each.

3.3 Gas-phase carbon

Model estimates are paired with hourly VOC (Figure S8) and mid-morning 3-hr average VOC (Figure S9) at both locations. Compounds considered largely fossil in origin including xylene, toluene, and benzene are generally well predicted at both sites although these species tend to be slightly overestimated at Pasadena and slightly underestimated at Bakersfield. Since emissions of these compounds near these sites are largely from mobile sources (Table 1), this suggests emissions from this sector are fairly well characterized in this application.

Contemporary (biogenic) origin monoterpenes are underestimated at both sites while isoprene is underestimated at Pasadena and has little bias at Bakersfield based on hourly measurements (Figure S8; Table 2). Isoprene and monoterpene performance may be partly related to the model not fully capturing transport from nearby areas with large emitting vegetation to these monitor locations (Heo et al., 2015), deficiencies in emissions factors, or poorly characterized vegetation. Speciated monoterpene measurements made at Bakersfield during this field campaign suggest emissions of certain species were elevated at the start of this time period due to flowering (Gentner et al., 2014b), which is a process not included in current biogenic emissions models and thus may contribute to modeled monoterpene underestimates.

Other VOC species that are systematically underestimated include ethane, methanol, ethanol, and acetaldehyde. Underprediction of methanol and ethanol in Bakersfield may be largely related to missing VOC emissions for confined animal operations in the emission inventory (Gentner et al., 2014a). Underestimates of oxygenated VOC compounds may indirectly impact SOC formation through muted photochemistry (Steiner et al., 2008). Carbon monoxide tends to be underestimated at both locations (Figure S8), possibly due to boundary inflow concentrations from the global model simulation being too low or underestimated regional emissions.

3.4 $PM_{2.5}$ SOC tracers

Figure 4 shows modeled and measured total PM2.5 OC mass. Measured mass explained by fossil and contemporary SOC tracers are shown in the top row. The unexplained observed fraction is a mixture of primary, secondary, fossil and contemporary origin. Modeled mass is colored to differentiate primarily emitted OC and SOC. Estimates of SOC mass from a specific or lumped VOC group (e.g. isoprene, monoterpenes, toluene), hereafter called SOC tracer mass, comprise little of the measured or modeled $PM_{2.5}$ OC at either of these locations during this field study (Figure 4). Total SOC tracer estimates explain only 9% of the total measured UNC/EPA $PM_{2.5}$ OC at Pasadena and 5% at Bakersfield. The percentage of mass explained by known secondary tracers is smaller than urban areas in the southeast United States: Atlanta 27% and Birmingham 31% (Kleindienst et al., 2010).

The portion of measured and modeled $PM_{2.5}$ carbon not identified with tracers may be from underestimated adjustment factors related to previously uncharacterized SVOC wall loss in chamber studies (Zhang et al., 2014b) and unidentified SOC pathways. Additional reasons for the low estimate of observed tracer contribution to PM2.5 carbon include known pathways without an ambient tracer and tracer degradation between formation and measurement. Based on ^{14}C measurements, this unidentified portion of the measurements is likely comprised of both contemporary and fossil carbon in generally similar amounts. Total modeled SOC explain only 12% of the $PM_{2.5}$ carbon at Bakersfield and 7% at Pasadena. As noted previously, AMS based observations suggest most OC is SOC (63%) at Pasadena (Hayes et al., 2013) meaning both the SOC tracer measurements and model estimates explain little of the SOC at this location.

Despite the relatively small component of $PM_{2.5}$ carbon explained by SOC tracers, a comparison of measured and modeled SOC and precursor VOC provides additional opportunity to better understand sources of $PM_{2.5}$ carbon in these areas and begin to establish relationships between precursors and resulting SOC formation. Ambient and model estimated SOC tracers and daily average VOC precursors are shown in Figure 5 for Pasadena and Figure 6 for Bakersfield. The model underestimates toluene and xylene SOC at both locations even though VOC gas precursors show an overprediction tendency at Pasadena and slight underestimation at Bakersfield. Isoprene SOC is generally under predicted at both sites, in particular at Bakersfield. This is in contrast to the slight overprediction of daily 24-hr average isoprene at Bakersfield. One explanation may be that isoprene SOC is formed elsewhere in the region (e.g. the nearby foothills of the Sierra Nevada where emissions are highest in the region), which would support the lack of relationship between isoprene SOC and isoprene concentrations at Bakersfield (Heo et al., 2015;Shilling et al., 2013). The lack of relationship could also be related to the reactive uptake kinetics of isoprene-derived epoxydiols (IEPOX) (Gaston et al., 2014) and methacrylic acid epoxide (MAE). Since the model does not include the reactive uptake of IEPOX and MAE and subsequent acid-catalyzed aqueous phase chemistry it is likely isoprene SOC would be underestimated to some degree at both sites (Karambelas et al., 2013;Pye et al., 2013). Of these channels the IEPOX channel is thought to have the largest SOA production potential, but the chemistry in the LA basin is dominated by the high-NO channel (Hayes et al., 2014) and thus IEPOX is not formed from isoprene emitted within the LA basin. Consistent with that observation, the AMS tracer of IEPOX SOA is only detected at background level in the LA basin.

Monoterpene VOC and monoterpene SOC are underestimated systematically at both locations suggesting underpredictions of the VOC precursor translates to underestimates in SOC. As noted previously, monoterpene measurements suggest an emissions enhancement related to flowering or other emission events (e.g. harvest or pruning) (Gentner et al., 2014b) that is not included in current biogenic emissions model formulations. The monoterpene measured tracer SOC group is based on α-pinene products. Measured SOC at these sites could be from monoterpene species other than α-pinene. A coincident study near Bakersfield indicates α- and β-pinene emissions represent a fairly small fraction of total monoterpene emissions during this time period (Gentner et al., 2014b). SOA yields in CMAQ for monoterpenes are heavily weighted toward α- and β- pinene, which may be appropriate in most places, but not here where measurements show large contributions from limonene, myrcene, and para-cymene. This is important because yields vary among from different monoterpenes and limonene has a much larger SOA yield than pinenes (Carlton et al., 2010).

Sesquiterpene VOC and SOC tracer (β-caryophyllenic acid) mass measurements were never above the MDL at either site during CalNex, but the modeling system often predicts SOC from this VOC group (Table 2, Figure S10b). The SOC tracer measurement methodology is more uncertain for sesquiterpene products (Offenberg et al., 2009) and gas-phase sesquiterpenes would have oxidized before reaching the measurement sites since sesquiterpene emitting vegetation exists in the San Joaquin Valley (Ormeño et al., 2010). It is also possible that SOC is forming from sesquiterpenes other than β-caryophyllene.

One potential explanation for an underestimation of SOC despite well characterized precursors (e.g. toluene and xylenes) could be lack of available oxidants. As shown in Figure 7, the model tends to overestimate the hydroxyl radical compared with measurement estimates at Pasadena. Hydroperoxyl+peroxy radical measurements are underestimated at Pasadena by a factor of 2 on average. The model overestimates preliminary measurements of both hydroxyl (by nearly a factor of 2 on average) and hydroperoxyl+peroxy radicals at Bakersfield. Model representation of hydroxyl radical at these locations during this time period does not seem to be limiting VOC oxidation to semi-volatile products. Better agreement between radical ambient and modeled estimates could result in less SOC produced by the model and exacerbate model SOC underestimates. This suggests deficiencies other than radical representation by the modeling system are more influential in SOC performance for these areas. However, hydroperoxyl underestimates at Pasadena could lead to muted SOA formation through low-NO_X pathways dependent on hydroperoxyl concentrations and contribute to model under-estimates of SOC.

3.5 Sensitivity Simulation

OH is not underestimated in the model and biases in precursor VOC do not clearly translate into similar biases in SOC (e.g. toluene and xylene VOC are overestimated at Pasadena but tracer SOC for this group is underestimated) for these sites during this time period. Modeled SOC may partly be underestimated due to the use of experimental SOC yields that may be biased low due to chamber studies not fully accounting for SVOC wall loss (Zhang et al., 2014b). Even though Zhang et al., 2014b showed results for one precursor to SOA pathway, as a sensitivity study here the yield of all semivolatile gases are increased by a factor of 4. This was done by increasing in the mass-based stoichiometric coefficients for each VOC to SOA pathway in the model to provide a preliminary indication about how increased yields might impact model performance. A factor of 4 is chosen based on the upper limit related to SVOC wall loss in Zhang et al. (Zhang et al., 2014b). Aside from wall loss characterization, there are a variety of other aspects of chamber studies that could result in underestimated yields including particle-phase accretion and aqueous phase chemistry and differences in chamber and ambient humidity.

Model estimates of $PM_{2.5}$ OC increase in urban areas and regionally when semivolatile yields are increased. The sensitivity simulation results in episode average anthropogenic SOC increases by a factor of 3 (benzene SOC at Pasadena) to 4.8 (toluene and xylene SOC at Pasadena) and biogenic SOC increases between a factor of 5.1 (isoprene SOC at Pasadena) to 8.9 (monoterpene SOC at

Bakersfield). Model performance improves at the CalNex locations (Figures 3 and 4) and at routine monitors throughout California (Figure 8). Average fractional bias improves from -34% to -11% at routine monitor locations and fractional error is reduced from 53% to 42%.

The sensitivity simulation with increased semivolatile yields results in increased model estimated secondary contribution as a percent of $PM_{2.5}$ carbon, but still does not conform to observation based estimates that indicate $PM_{2.5}$ carbon is largely secondary in nature at these sites (Liu et al., 2012;Hayes et al., 2013). Modeled SOC in the sensitivity simulation explains 36% of the $PM_{2.5}$ OC at Bakersfield and 22% at Pasadena, which is larger than the baseline simulation by more than a factor of 3. The model predicted percent contemporary fraction of $PM_{2.5}$ carbon changed very little due to this sensitivity. The model sensitivity results are not compared to SOC tracer group estimates since the conversion of tracer concentrations to SOC concentrations would require a similar adjustment and would result in similar relationships between model estimates and observations.

3.6 Aqueous and other SOC processes

Measurements in Pasadena during the summer of 2009 suggest aqueous processes can be important for SOC mass (Hersey et al., 2011). For the CalNex period at Pasadena, Washenfelder et al. (2012) showed box model estimated 8-hr average SOC from aqueous-phase chemistry of glyoxal to be between 0.0 and 0.2 $\mu g\ m^{-3}$ (Washenfelder et al., 2011) and Hayes et al. (2014) showed that the observed SOA was not different between cloudy and clear morning days. CMAQ predicted 24-hour average SOC from glyoxal and methygloxal through aqueous chemistry at Pasadena ranges from 0.0 to 0.04 μg/m^3. CMAQ estimates of SOC from small carbonyl compounds via aqueous-phase processes are within the range inferred from measurements.

Not all CMAQ SOC formation pathways can be included in this analysis. No observational indicator exists for SOC derived from alkanes, benzene, glyoxal, and methylglyoxal since unique tracer species have not been determined. Conversely, naphthalene/PAH SOC tracers were measured, but not modeled in CMAQ. Measured naphthalene SOC at these sites is minor (Hayes et al., 2014) which is consistent with other areas (Dzepina et al., 2009). Previous CMAQ simulations predict that PAHs contribute less than 30 ng m^{-3} of SOA in Southern California in summer (Pye and Pouliot, 2012), and thus including those pathways is unlikely to close the model-measurement gap in PM2.5 OC. 2-Methyl-3-Buten-2-ol (MBO) derived SOC concentrations (3-4 ngC m^{-3}) were low at both monitor locations throughout the campaign (Lewandowski et al., 2013). MBO does not appear to notably contribute SOC at these locations during this time period, which is consistent with low yields estimated in laboratory experiments (Chan et al., 2009). Organic carbon emitted from marine biological activity is not included in this modeling assessment and may contribute to some degree at Pasadena (Gantt et al., 2010) based on ship-based measurements (Hayes et al., 2013).

3.7 Regional $PM_{2.5}$ Organic Carbon

Including routine measurement data is important to provide broader context for $PM_{2.5}$ carbon in California and understand how the model performs and responds to perturbations at diverse locations beyond the two CalNex sites. The highest average modeled $PM_{2.5}$ OC in California during this period is in the Los Angeles area (Figure 8). The Sacramento and San Joaquin valleys also show higher concentrations of $PM_{2.5}$ OC than more rural parts of the State (Figure 8). Measurements made at routine monitor networks (Figure 8) show similar elevated concentrations near Los Angeles, Sacramento valley, and San Joaquin valley. These areas of elevated OC generally coincide with areas of the State that experience a build-up of pollutants due to terrain features blocking air flow (Baker et al., 2013). The model does not tend to capture the highest concentrations of measured $PM_{2.5}$ OC in the central San Joaquin valley, Imperial Valley, or at one CSN monitor in the northeast Sierra Nevada that is near large residential wood combustion emissions (Figure S11). The model underestimates $PM_{2.5}$ OC on average across all CSN sites during this time period (fractional bias = -34% and fractional error = 53%). The modeling systems show an overprediction tendency (fractional bias = 77%) across all CSN sites for $PM_{2.5}$ elemental carbon in California during this period.

4 Conclusions

Total $PM_{2.5}$ carbon at Pasadena and Bakersfield during the CalNex period in May and June of 2010 is fairly evenly split between contemporary and fossil origin. Total $PM_{2.5}$ OC is generally underestimated at both field study locations and at many routine measurement sites in California and comparison with AMS observations suggest a large underestimation of SOC. Semivolatile yields were increased by a factor of 4 based on recent research suggesting yields may be higher due to updated accounting for SVOC wall loss. This sensitivity resulted in a better comparison to routine and field study measurements. However, the model estimated OC is still largely primary in nature and inconsistent with observation based approaches at these sites. A modeling study for the same time period using different emissions, photochemical transport model, and SOA treatment also show underestimated OA and SOA at Pasadena and underestimated SOA but comparable OA at the Bakersfield location (Fast et al., 2014).

CMAQ predictions of individual VOCs are often not consistent with model performance for the corresponding subsequent SOC species mass. Gas-phase mixing ratios of toluene and xylene are well-predicted by CMAQ, typically within a factor of 2 of the observations at both sites. However, measurement-based estimates of the corresponding SOC mass are consistently greater than model-predicted mass. Mass concentrations of the isoprene SOC are systematically underpredicted, most noticeably at Bakersfield, while model predictions of gas-phase isoprene are not biased in only one direction to the same degree. Gas-phase monoterpenes and the related SOC species are underpredicted at both CalNex monitoring sites. The hydroxyl radical is fairly well characterized at Pasadena and systematically overestimated at Bakersfield suggesting oxidants are not limiting SOC production in the model.

Episode average CMAQ model estimates of $PM_{2.5}$ OC contemporary fraction at Pasadena and Bakersfield are similar to radiocarbon measurements but lack day to day variability. CMAQ $PM_{2.5}$ OC is predominantly primary in origin which is contrary to findings from other studies that $PM_{2.5}$ OC in these areas are largely secondary in nature during this time period (Bahreini et al., 2012;Hayes et al., 2013;Liu et al., 2012). Treatment of primarily emitted $PM_{2.5}$ OC as semi-volatile would likely result in total $PM_{2.5}$ OC estimates that would be mostly secondary rather than primary. However, this would likely exacerbate model underestimates of PM2.5 OC. Some model performance features including underestimated SOC may be related to less volatile hydrocarbon emissions missing from the emission inventory (Chan et al., 2013;Gentner et al., 2012;Jathar et al., 2014;Zhao et al., 2014) or mischaracterized when lumped into chemical mechanism VOC species (Jathar et al., 2014). A future intent is to simulate this same period using a volatility basis set approach to treat primary OC emissions with some degree of volatility and potential for SOC production and better account for sector specific intermediate volatility emissions.

Disclaimer

Although this work was reviewed by EPA and approved for publication, it may not necessarily reflect official Agency policy.

Acknowledgements

The authors would like to acknowledge measurements taken by Scott Scheller and the contribution from Chris Misenis, Allan Beidler, Chris Allen, James Beidler, Heather Simon, and Rich Mason. EPA, through its Office of Research and Development, funded and collaborated in the research described here under Contract EP-D-10-070 to Alion Science and Technology. This work is supported in part through EPA's STAR program, grant number RD83504101. PLH and JLJ were supported by CARB 11-305.

Supporting Information

Additional measurement methods, model description, model output, and comparison with measurements and formulas used for data pairing are provided in the Supporting Information.

References

Bahreini, R., Middlebrook, A. M., de Gouw, J. A., Warneke, C., Trainer, M., Brock, C. A., Stark, H., Brown, S. S., Dube, W. P., Gilman, J. B., Hall, K., Holloway, J. S., Kuster, W. C., Perring, A. E., Prevot, A. S. H., Schwarz, J. P., Spackman, J. R., Szidat, S., Wagner, N. L., Weber, R. J., Zotter, P., and Parrish, D. D.: Gasoline emissions dominate over diesel in formation of secondary organic aerosol mass, Geophysical Research Letters, 39, 10.1029/2011gl050718, 2012.

Baker, K. R., Misenis, C., Obland, M. D., Ferrare, R. A., Scarino, A. J., and Kelly, J. T.: Evaluation of surface and upper air fine scale WRF meteorological modeling of the May and June 2010 CalNex period in California, Atmospheric Environment, 80, 299-309, 2013.

Barsanti, K., Carlton, A., and Chung, S.: Analyzing experimental data and model parameters: implications for predictions of SOA using chemical transport models, Atmospheric Chemistry and Physics, 13, 12073-12088, 2013.

Birch, M., and Cary, R.: Elemental carbon-based method for monitoring occupational exposures to particulate diesel exhaust, Aerosol Science and Technology, 25, 221-241, 1996.

Borbon, A., Gilman, J., Kuster, W., Grand, N., Chevaillier, S., Colomb, A., Dolgorouky, C., Gros, V., Lopez, M., and Sarda-Esteve, R.: Emission ratios of anthropogenic volatile organic compounds in northern mid-latitude megacities: Observations versus emission inventories in Los Angeles and Paris, Journal of Geophysical Research: Atmospheres, 118, 2041-2057, 2013.

Carlton, A. G., Turpin, B. J., Altieri, K. E., Reff, A., Seitzinger, S., Lim, H. J., and Ervens, B.: Atmospheric Oxalic Acid and SOA Production from Glyoxal: Results of Aqueous Photooxidation Experiments, Atmospheric Environment, 41, 7588-7602, 2007.

Carlton, A. G., Turpin, B. J., Altieri, K. E., Seitzinger, S. P., Mathur, R., Roselle, S. J., and Weber, R. J.: CMAQ model performance enhanced when in-cloud SOA is included: comparisons of OC predictions with measurements, Environ. Sci. Technol., 42, 8798-8802, 2008.

Carlton, A. G., Bhave, P. V., Napelenok, S. L., Edney, E. O., Sarwar, G., Pinder, R. W., Pouliot, G. A., and Houyoux, M.: Treatment of secondary organic aerosol in CMAQv4.7, Environmental Science and Technology, 44, 8553-8560, 2010.

Carlton, A. G., and Baker, K. R.: Photochemical Modeling of the Ozark Isoprene Volcano: MEGAN, BEIS, and Their Impacts on Air Quality Predictions, Environmental Science & Technology, 45, 4438-4445, 10.1021/es200050x, 2011.

Carter, W. P. L.: Implementation of the SAPRC-99 chemical mechanism into the models-3 framework, U.S. Environmental Protection Agency, University of California, Riverside, CA, USA, 2000.

Chan, A. W., Isaacman, G., Wilson, K. R., Worton, D. R., Ruehl, C. R., Nah, T., Gentner, D. R., Dallmann, T. R., Kirchstetter, T. W., and Harley, R. A.: Detailed chemical characterization of unresolved complex mixtures in atmospheric organics: Insights into emission sources, atmospheric processing, and secondary organic aerosol formation, Journal of Geophysical Research: Atmospheres, 118, 6783-6796, 2013.

Chan, A. W. H., Galloway, M. M., Kwan, A. J., Chhabra, P. S., Keutsch, F. N., Wennberg, P. O., Flagan, R. C., and Seinfeld, J. H.: Photooxidation of 2-Methyl-3-Buten-2-ol (MBO) as a Potential Source of Secondary Organic Aerosol, Environmental Science & Technology, 43, 4647-4652, 10.1021/es802560w, 2009.

Chow, J. C., Watson, J. G., Crow, D., Lowenthal, D. H., and Merrifield, T.: Comparison of IMPROVE and NIOSH carbon measurements, Aerosol Science & Technology, 34, 23-34, 2001.

Chung, S. H., and Seinfeld, J. H.: Global distribution and climate forcing of carbonaceous aerosols, Journal of Geophysical Research-Atmospheres, 107, AAC 14.11-AAC 14-33, 10.1029/2001jd001397, 2002.

Docherty, K. S., Stone, E. A., Ulbrich, I. M., DeCarlo, P. F., Snyder, D. C., Schauer, J. J., Peltier, R. E., Weber, R. J., Murphy, S. N., Seinfeld, J. H., Grover, B. D., Eatough, D. J., and Jiimenez, J. L.: Apportionment of Primary and Secondary Organic Aerosols in Southern California during the 2005 Study of Organic Aerosols in Riverside (SOAR-1), Environmental Science & Technology, 42, 7655-7662, 10.1021/es8008166, 2008.

Dusanter, S., Vimal, D., Stevens, P., Volkamer, R., and Molina, L.: Measurements of OH and HO 2 concentrations during the MCMA-2006 field campaign–Part 1: Deployment of the Indiana University laser-induced fluorescence instrument, Atmospheric Chemistry and Physics, 9, 1665-1685, 2009.

Dzepina, K., Volkamer, R. M., Madronich, S., Tulet, P., Ulbrich, I. M., Zhang, Q., Cappa, C. D., Ziemann, P. J., and Jimenez, J. L.: Evaluation of recently-proposed secondary organic aerosol models for a case study in Mexico City, Atmospheric Chemistry and Physics, 9, 5681-5709, 2009.

Edney, E. O., Kleindienst, T. E., Conver, T. S., McIver, C. D., Corse, E. W., and Weathers, W. S.: Polar organic oxygenates in PM2.5 at a southeastern site in the United States, Atmospheric Environment, 37, 3947-3965, 2003.

Ensberg, J., Hayes, P., Jimenez, J., Gilman, J., Kuster, W., de Gouw, J., Holloway, J., Gordon, T., Jathar, S., and Robinson, A.: Emission factor ratios, SOA mass yields, and the impact of vehicular emissions on SOA formation, Atmospheric Chemistry and Physics, 14, 2383-2397, 2014.

Ervens, B., Turpin, B., and Weber, R.: Secondary organic aerosol formation in cloud droplets and aqueous particles (aqSOA): a review of laboratory, field and model studies, Atmospheric Chemistry and Physics, 11, 11069-11102, 2011.

Fast, J., Allan, J., Bahreini, R., Craven, J., Emmons, L., Ferrare, R., Hayes, P., Hodzic, A., Holloway, J., and Hostetler, C.: Modeling regional aerosol and aerosol precursor variability over California and its sensitivity to emissions and long-range transport during the 2010 CalNex and CARES campaigns, Atmospheric Chemistry and Physics, 14, 10013-10060, 2014.

Fountoukis, C., and Nenes, A.: ISORROPIA II: a computationally efficient thermodynamic equilibrium model for K+-Ca2+-Mg2+-Nh(4)(+)-Na+-SO42--NO3--Cl--H2O aerosols, Atmospheric Chemistry and Physics, 7, 4639-4659, 2007.

Gantt, B., Meskhidze, N., and Carlton, A.: The contribution of marine organics to the air quality of the western United States, Atmospheric Chemistry and Physics, 10, 7415-7423, 2010.

Gaston, C. J., Riedel, T. P., Zhang, Z., Gold, A., Surratt, J. D., and Thornton, J. A.: Reactive Uptake of an Isoprene-derived Epoxydiol to Submicron Aerosol Particles, Environmental science & technology, 48, 11178-11186, 10.1021/es5034266, 2014.

Gentner, D., Ford, T., Guha, A., Boulanger, K., Brioude, J., Angevine, W., de Gouw, J., Warneke, C., Gilman, J., and Ryerson, T.: Emissions of organic carbon and methane from petroleum and dairy operations in California's San Joaquin Valley, Atmospheric Chemistry and Physics, 14, 4955-4978, doi:10.5194/acp-14-4955-2014, 2014a.

Gentner, D., Ormeño, E., Fares, S., Ford, T., Weber, R., Park, J.-H., Brioude, J., Angevine, W., Karlik, J., and Goldstein, A.: Emissions of terpenoids, benzenoids, and other biogenic gas-phase organic compounds from agricultural crops and their potential implications for air quality, Atmospheric Chemistry and Physics, 14, 5393-5413, 2014b.

Gentner, D. R., Isaacman, G., Worton, D. R., Chan, A. W. H., Dallmann, T. R., Davis, L., Liu, S., Day, D. A., Russell, L. M., Wilson, K. R., Weber, R., Guha, A., Harley, R. A., and Goldstein, A. H.: Elucidating secondary organic aerosol from diesel and gasoline vehicles through detailed characterization of organic carbon emissions, Proceedings of the National Academy of Sciences of the United States of America, 109, 18318-18323, 10.1073/pnas.1212272109, 2012.

Gerbig, C., Schmitgen, S., Kley, D., Volz-Thomas, A., Dewey, K., and Haaks, D.: An improved fast-response vacuum-UV resonance fluorescence CO instrument, Journal of Geophysical Research: Atmospheres (1984–2012), 104, 1699-1704, 1999.

Geron, C.: Carbonaceous aerosol over a< i> Pinus taeda</i> forest in Central North Carolina, USA, Atmospheric Environment, 43, 959-969, 2009.

Gilman, J., Burkhart, J., Lerner, B., Williams, E., Kuster, W., Goldan, P., Murphy, P., Warneke, C., Fowler, C., and Montzka, S.: Ozone variability and halogen oxidation within the Arctic and sub-Arctic springtime boundary layer, Atmospheric Chemistry and Physics Discussions, 10, 15885-15919, 2010.

Grell, G. A., Peckham, S. E., Schmitz, R., McKeen, S. A., Frost, G., Skamarock, W. C., and Eder, B.: Fully coupled "online" chemistry within the WRF model, Atmospheric Environment, 39, 6957-6975, 10.1016/j.atmosenv.2005.04.027, 2005.

Griffith, S., Hansen, R., Dusanter, S., Stevens, P., Alaghmand, M., Bertman, S., Carroll, M., Erickson, M., Galloway, M., and Grossberg, N.: OH and HO 2 radical chemistry during PROPHET 2008 and CABINEX 2009–Part 1: Measurements and model comparison, Atmospheric Chemistry and Physics, 13, 5403-5423, 2013.

Hallquist, M., Wenger, J. C., Baltensperger, U., Rudich, Y., Simpson, D., Claeys, M., Dommen, J., Donahue, N. M., George, C., Goldstein, A. H., Hamilton, J. F., Herrmann, H., Hoffmann, T., Iinuma, Y., Jang, M., Jenkin, M. E., Jimenez, J. L., Kiendler-Scharr, A., Maenhaut, W., McFiggans, G., Mentel, T. F., Monod, A., Prevot, A. S. H., Seinfeld, J. H., Surratt, J. D., Szmigielski, R., and Wildt, J.: The formation, properties and impact of secondary organic aerosol: current and emerging issues, Atmospheric Chemistry and Physics, 9, 5155-5236, 2009.

Hayes, P. L., Ortega, A. M., Cubison, M. J., Froyd, K. D., Zhao, Y., Cliff, S. S., Hu, W. W., Toohey, D. W., Flynn, J. H., Lefer, B. L., Grossberg, N., Alvarez, S., Rappenglueck, B., Taylor, J. W., Allan, J. D., Holloway, J. S., Gilman, J. B., Kuster, W. C., De Gouw, J. A., Massoli, P., Zhang, X., Liu, J., Weber, R. J., Corrigan, A. L., Russell, L. M., Isaacman, G., Worton, D. R., Kreisberg, N. M., Goldstein, A. H., Thalman, R., Waxman, E. M., Volkamer, R., Lin, Y. H., Surratt, J. D., Kleindienst, T. E., Offenberg, J. H., Dusanter, S., Griffith, S., Stevens, P. S., Brioude, J., Angevine, W. M., and Jimenez, J. L.: Organic aerosol composition and sources in Pasadena, California, during the 2010 CalNex campaign, Journal of Geophysical Research-Atmospheres, 118, 9233-9257, 10.1002/jgrd.50530, 2013.

Hayes, P. L., Carlton, A. G., Baker, K. R., Ahmadov, R., Washenfelder, R. A., Alvarez, S., Rappenglueck, B., Gilman, J. B., Kuster, W. C., De Gouw, J. A., Zotter, P., Prevot, A. S. H., Szidat, S., Kleindienst, T. E., Offenberg, J. H., and Jimenez, J. L.: Modeling the formation and aging of secondary organic aerosols in Los Angeles during CalNex 2010, Atmospheric Chemistry and Physics Discussions, 2014.

Henderson, B., Akhtar, F., Pye, H., Napelenok, S., and Hutzell, W.: A database and tool for boundary conditions for regional air quality modeling: description and evaluation, Geoscientific Model Development, 7, 339-360, 2014.

Henze, D. K., and Seinfeld, J. H.: Global secondary organic aerosol from isoprene oxidation, Geophysical Research Letters, 33, L09812, 10.1029/2006gl025976, 2006.

Heo, J., de Foy, B., Olson, M. R., Pakbin, P., Sioutas, C., and Schauer, J. J.: Impact of regional transport on the anthropogenic and biogenic secondary organic aerosols in the Los Angeles Basin, Atmospheric Environment, 103, 171-179, 2015.

Hersey, S. P., Craven, J. S., Schilling, K. A., Metcalf, A. R., Sorooshian, A., Chan, M. N., Flagan, R. C., and Seinfeld, J. H.: The Pasadena Aerosol Characterization Observatory (PACO): chemical and physical analysis of the Western Los Angeles basin aerosol, Atmospheric Chemistry and Physics, 11, 7417-7443, 10.5194/acp-11-7417-2011, 2011.

Hutzell, W. T., Luecken, D. J., Appel, K. W., and Carter, W. P. L.: Interpreting predictions from the SAPRC07 mechanism based on regional and continental simulations, Atmospheric Environment, 46, 417-429, 10.1016/j.atmosenv.2011.09.030, 2012.

Jathar, S. H., Gordon, T. D., Hennigan, C. J., Pye, H. O. T., Pouliot, G., Adams, P. J., Donahue, N. M., and Robinson, A. L.: Unspeciated organic emissions from combustion sources and their influence on the secondary organic aerosol budget in the United States, Proceedings of the National Academy of Sciences, 111, 10473-10478, 10.1073/pnas.1323740111, 2014.

Jimenez, J. L., Canagaratna, M. R., Donahue, N. M., Prevot, A. S. H., Zhang, Q., Kroll, J. H., DeCarlo, P. F., Allan, J. D., Coe, H., Ng, N. L., Aiken, A. C., Docherty, K. S., Ulbrich, I. M., Grieshop, A. P., Robinson, A. L., Duplissy, J., Smith, J. D., Wilson, K. R., Lanz, V. A., Hueglin, C., Sun, Y. L., Tian, J., Laaksonen, A., Raatikainen, T., Rautiainen, J., Vaattovaara, P., Ehn, M., Kulmala, M., Tomlinson, J. M., Collins, D. R., Cubison, M. J., Dunlea, E. J., Huffman, J. A., Onasch, T. B., Alfarra, M. R., Williams, P. I., Bower, K., Kondo, Y., Schneider, J., Drewnick, F., Borrmann, S., Weimer, S., Demerjian, K., Salcedo, D., Cottrell, L., Griffin, R., Takami, A., Miyoshi, T., Hatakeyama, S., Shimono, A., Sun, J. Y., Zhang, Y. M., Dzepina, K., Kimmel, J. R., Sueper, D., Jayne, J. T., Herndon, S. C., Trimborn, A. M., Williams, L. R., Wood, E. C., Middlebrook, A. M., Kolb, C. E., Baltensperger, U., and Worsnop, D. R.: Evolution of Organic Aerosols in the Atmosphere, Science, 326, 1525-1529, 10.1126/science.1180353, 2009.

Karambelas, A., Pye, H. O. T., Budisulistiorini, S. H., Surratt, J. D., and Pinder, R. W.: Isoprene epoxydiol contribution to urban organic aerosol: evidence from modeling and measurements, Environmental Science & Technology Letters, 1, 278-283, 10.1021/ez5001353, 2013.

Kelly, J. T., Baker, K. R., Nowak, J. B., Murphy, J. G., Markovic, M. Z., VandenBoer, T. C., Ellis, R. A., Neuman, J. A., Weber, R. J., and Roberts, J. M.: Fine-scale simulation of ammonium and nitrate over the South Coast Air Basin and San Joaquin Valley of California during CalNex-2010, Journal of Geophysical Research: Atmospheres, 119, 3600-3614, 10.1002/2013JD021290, 2014.

Kleindienst, T. E., Conver, T. S., McIver, C. D., and Edney, E. O.: Determination of secondary organic aerosol products from the photooxidation of toluene and their implications in ambient PM2.5, Journal of Atmospheric Chemistry, 47, 79-100, 2004.

Kleindienst, T. E., Jaoui, M., Lewandowski, M., Offenberg, J. H., Lewis, C. W., Bhave, P. V., and Edney, E. O.: Estimates of the contributions of biogenic and anthropogenic hydrocarbons to secondary organic aerosol at a southeastern US location, Atmospheric Environment, 41, 8288-8300, 10.1016/j.atmosenv.2007.06.045, 2007.

Kleindienst, T. E., Lewandowski, M., Offenberg, J. H., Edney, E. O., Jaoui, M., Zheng, M., Ding, X. A., and Edgerton, E. S.: Contribution of Primary and Secondary Sources to Organic Aerosol and PM2.5 at SEARCH Network Sites, Journal of the Air & Waste Management Association, 60, 1388-1399, 10.3155/1047-3289.60.11.1388, 2010.

Lewandowski, M., Piletic, I. R., Kleindienst, T. E., Offenberg, J. H., Beaver, M. R., Jaoui, M., Docherty, K. S., and Edney, E. O.: Secondary organic aerosol characterisation at field sites across the United States during the spring–summer period, International Journal of Environmental Analytical Chemistry, 93, 1084-1103, 2013.

Lewis, C. W., Klouda, G. A., and Ellenson, W. D.: Radiocarbon measurement of the biogenic contribution to summertime PM-2.5 ambient aerosol in Nashville, TN, Atmospheric Environment, 38, 6053-6061, 10.1016/j.atmosenv.2004.06.011, 2004.

Liu, S., Ahlm, L., Day, D. A., Russell, L. M., Zhao, Y., Gentner, D. R., Weber, R. J., Goldstein, A. H., Jaoui, M., Offenberg, J. H., Kleindienst, T. E., Rubitschun, C., Surratt, J. D., Sheesley, R. J., and Scheller, S.: Secondary organic aerosol formation from fossil fuel sources contribute majority of summertime organic mass at Bakersfield, Journal of Geophysical Research-Atmospheres, 117, 10.1029/2012JD018170, 2012.

Mao, J., Ren, X., Zhang, L., Van Duin, D., Cohen, R., Park, J.-H., Goldstein, A., Paulot, F., Beaver, M., and Crounse, J.: Insights into hydroxyl measurements and atmospheric oxidation in a California forest, Atmospheric Chemistry and Physics, 12, 8009-8020, 2012.

Markovic, M., VandenBoer, T., Baker, K., Kelly, J., and Murphy, J.: Measurements and modeling of the inorganic chemical composition of fine particulate matter and associated precursor gases in California's San Joaquin Valley during CalNex 2010, Journal of Geophysical Research: Atmospheres, 119, 6853-6866, 10.1002/2013JD021408, 2014.

Offenberg, J. H., Lewandowski, M., Edney, E. O., Kleindienst, T. E., and Jaoui, M.: Influence of Aerosol Acidity on the Formation of Secondary Organic Aerosol from Biogenic Precursor Hydrocarbons, Environmental Science & Technology, 43, 7742-7747, 10.1021/es901538e, 2009.

Ormeño, E., Gentner, D. R., Fares, S., Karlik, J., Park, J. H., and Goldstein, A. H.: Sesquiterpenoid emissions from agricultural crops: correlations to monoterpenoid emissions and leaf terpene content, Environmental science & technology, 44, 3758-3764, 2010.

Pye, H. O., Pinder, R. W., Piletic, I. R., Xie, Y., Capps, S. L., Lin, Y.-H., Surratt, J. D., Zhang, Z., Gold, A., and Luecken, D. J.: Epoxide pathways improve model predictions of isoprene markers and reveal key role of acidity in aerosol formation, Environmental science & technology, 47, 11056-11064, 2013.

Pye, H. O. T., and Pouliot, G. A.: Modeling the Role of Alkanes, Polycyclic Aromatic Hydrocarbons, and Their Oligomers in Secondary Organic Aerosol Formation, Environmental Science & Technology, 46, 6041-6047, 10.1021/es300409w, 2012.

Robinson, A. L., Donahue, N. M., Shrivastava, M. K., Weitkamp, E. A., Sage, A. M., Grieshop, A. P., Lane, T. E., Pierce, J. R., and Pandis, S. N.: Rethinking organic aerosols: Semivolatile emissions and photochemical aging, Science, 315, 1259-1262, 2007.

Rollins, A., Browne, E., Min, K.-E., Pusede, S., Wooldridge, P., Gentner, D., Goldstein, A., Liu, S., Day, D., and Russell, L.: Evidence for NOx control over nighttime SOA formation, Science, 337, 1210-1212, 2012.

Ryerson, T. B., Andrews, A. E., Angevine, W. M., Bates, T. S., Brock, C. A., Cairns, B., Cohen, R. C., Cooper, O. R., de Gouw, J. A., Fehsenfeld, F. C., Ferrare, R. A., Fischer, M. L., Flagan, R. C., Goldstein, A. H., Hair, J. W., Hardesty, R. M., Hostetler, C. A., Jimenez, J. L., Langford, A. O., McCauley, E., McKeen, S. A., Molina, L. T., Nenes, A., Oltmans, S. J., Parrish, D. D., Pederson, J. R., Pierce, R. B., Prather, K., Quinn, P. K., Seinfeld, J. H., Senff, C. J., Sorooshian, A., Stutz, J., Surratt, J. D., Trainer, M., Volkamer, R., Williams, E. J., and Wofsy, S. C.: The 2010 California Research at the Nexus of Air Quality and Climate Change (CalNex) field study, Journal of Geophysical Research-Atmospheres, 118, 5830-5866, 10.1002/jgrd.50331, 2013.

Sarwar, G., Fahey, K., Kwok, R., Gilliam, R. C., Roselle, S. J., Mathur, R., Xue, J., Yu, J., and Carter, W. P. L.: Potential impacts of two SO2 oxidation pathways on regional sulfate concentrations: Aqueous-phase oxidation by NO2 and gas-phase oxidation by Stabilized Criegee Intermediates, Atmospheric Environment, 68, 186-197, 10.1016/j.atmosenv.2012.11.036, 2013.

Shilling, J. E., Zaveri, R. A., Fast, J. D., Kleinman, L., Alexander, M., Canagaratna, M. R., Fortner, E., Hubbe, J. M., Jayne, J. T., and Sedlacek, A.: Enhanced SOA formation from mixed anthropogenic and biogenic emissions during the CARES campaign, Atmospheric Chemistry and Physics, 13, 2091-2113, 2013.

Simon, H., and Bhave, P. V.: Simulating the Degree of Oxidation in Atmospheric Organic Particles, Environmental Science & Technology, 46, 331-339, 10.1021/es202361w, 2012.

Steiner, A. L., Cohen, R., Harley, R., Tonse, S., Millet, D., Schade, G., and Goldstein, A.: VOC reactivity in central California: comparing an air quality model to ground-based measurements, Atmospheric Chemistry and Physics, 8, 351-368, 2008.

Stroud, C. A., Liggio, J., Zhang, J., Gordon, M., Staebler, R. M., Makar, P. A., Zhang, J., Li, S. M., Mihele, C., and Lu, G.: Rapid organic aerosol formation downwind of a highway: Measured and model results from the FEVER study, Journal of Geophysical Research: Atmospheres, 119, 1663-1679, 2014.

Stuiver, M.: International agreements and the use of the new oxalic acid standard, Radiocarbon, 25, 793-795, 1983.

Tan, Y., Carlton, A. G., Seitzinger, S. P., and Turpin, B. J.: SOA from methylglyoxal in clouds and wet aerosols: measurement and prediction of key products, Atmospheric Environment, 44, 5218-5226, 10.1016/j.atmosenv.2010.08.045, 2010.

http://www.epa.gov/ttn/chief/net/2011nei/2011_neiv1_tsd_draft.pdf. Accessed October 1, 2014.: ftp://ftp.epa.gov/EmisInventory/2001v2CAP/2001emis/readme_2001emis.txt, access: October 2, 2014, 2014.

Wagstrom, K. M., Baker, K. R., Leinbach, A. E., and Hunt, S. W.: Synthesizing Scientific Progress: Outcomes from US EPA's Carbonaceous Aerosols and Source Apportionment STAR Grants, Environmental science & technology, 48, 10561-10570, 2014.

Washenfelder, R. A., Young, C. J., Brown, S. S., Angevine, W. M., Atlas, E. L., Blake, D. R., Bon, D. M., Cubison, M. J., de Gouw, J. A., Dusanter, S., Flynn, J., Gilman, J. B., Graus, M., Griffith, S., Grossberg, N., Hayes, P. L., Jimenez, J. L., Kuster, W. C., Lefer, B. L., Pollack, I. B., Ryerson, T. B., Stark, H., Stevens, P. S., and Trainer, M. K.: The glyoxal budget and its contribution to organic aerosol for Los Angeles, California, during CalNex 2010, Journal of Geophysical Research-Atmospheres, 116, 10.1029/2011jd016314, 2011.

Yarwood, G., Rao, S., Yocke, M., and Whitten, G. Z.: Updates to the carbon bond chemical mechanism: CB05, ENVIRON International Corporation, Novato, CA, 2005.

Zhang, H., Chen, G., Hu, J., Chen, S.-H., Wiedinmyer, C., Kleeman, M., and Ying, Q.: Evaluation of a seven-year air quality simulation using the Weather Research and Forecasting (WRF)/Community Multiscale Air Quality (CMAQ) models in the eastern United States, Science of The Total Environment, 473, 275-285, 2014a.

Zhang, X., Cappa, C. D., Jathar, S. H., McVay, R. C., Ensberg, J. J., Kleeman, M. J., and Seinfeld, J. H.: Influence of vapor wall loss in laboratory chambers on yields of secondary organic aerosol, Proceedings of the National Academy of Sciences, 111, 5802-5807, 2014b.

Zhao, Y., Kreisberg, N. M., Worton, D. R., Isaacman, G., Gentner, D. R., Chan, A. W., Weber, R. J., Liu, S., Day, D. A., and Russell, L. M.: Sources of organic aerosol investigated using organic compounds as tracers measured during CalNex in Bakersfield, Journal of Geophysical Research: Atmospheres, 118, 11388-11398, 2013.

Zhao, Y., Hennigan, C. J., May, A. A., Tkacik, D. S., de Gouw, J. A., Gilman, J. B., Kuster, W. C., Borbon, A., and Robinson, A. L.: Intermediate-Volatility Organic Compounds: A Large Source of Secondary Organic Aerosol, Environmental science & technology, 48, 13743-13750, 2014.

Zotter, P., El-Haddad, I., Zhang, Y., Hayes, P. L., Zhang, X., Lin, Y. H., Wacker, L., Schnelle-Kreis, J., Abbaszade, G., and Zimmermann, R.: Diurnal cycle of fossil and nonfossil carbon using radiocarbon analyses during CalNex, Journal of Geophysical Research: Atmospheres, 119, 6818-6835, 10.1002/2013JD021114, 2014.

Table 1. Episode total anthropogenic emissions of primarily emitted PM2.5 organic carbon and the sum of benzene, toluene, and xylenes by emissions sector group. The Los Angeles (LA) total includes Los Angeles and Orange counties. The southern San Joaquin Valley (SSJV) total includes Kern, Fresno, Kings, and Tulare counties. Residential wood combustion, fugitives, and non-point area PM2.5 emissions are largely contemporary in origin.

	Primarily emitted PM2.5 organic carbon				Benzene + Toluene + Xylenes			
Sector	SSJV (tons)	SSJV (%)	LA (tons)	LA (%)	SSJV (tons)	SSJV (%)	LA (tons)	LA (%)
Non-point area	139.9	33.8	410.1	40.8	326.7	37.2	1229.3	35.8
Onroad mobile	73.3	17.7	263.6	26.2	273.5	31.2	1190.9	34.6
Nonroad mobile	23.9	5.8	161.4	16.1	170.1	19.4	822.3	23.9
Point: non-electrical generating	61.3	14.8	56.3	5.6	68.3	7.8	177.7	5.2
Residential wood combustion	54.1	13.1	82.7	8.2	2.0	0.2	3.2	0.1
Oil & gas exploration and related	28.5	6.9	0.0	0.0	34.2	3.9	1.1	0.0
Fugitive dust	24.9	6.0	18.1	1.8	0.0	0.0	0.0	0.0
Commercial marine & rail	3.8	0.9	11.4	1.1	2.6	0.3	12.8	0.4
Point: electrical generating	4.3	1.0	1.7	0.2	0.1	0.0	1.0	0.0
Total Contemporary Carbon	218.9	52.9	510.9	50.8	2.0	0.2	3.2	0.1
Total Fossil Carbon	195.2	47.1	494.5	49.2	875.3	99.8	3435.1	99.9

Table 2. Episode average measured and modeled PM2.5 carbon, PM2.5 SOC groups, and VOC at the Pasadena and Bakersfield sites.

Specie	Model Run	Location	N	Observed (ugC/m3)	Predicted (ugC/m3)	Bias (ugC/m3)	Error (ugC/m3)	Fractional Bias (%)	Fractional Error (%)	r
Elemental Carbon	Baseline	Bakersfield	35	0.5	0.4	-0.1	0.1	-13	35	0.17
	Baseline	Pasadena	31	0.2	1.0	0.8	0.8	125	125	0.70
	Baseline	CSN/IMPROVE sites	220	0.2	0.6	0.6	0.6	77	87	0.47
Organic Carbon	Baseline	Bakersfield	35	5.4	0.8	-4.6	4.6	-144	144	0.11
	Baseline	Pasadena	31	3.6	2.0	-1.6	1.6	-53	53	0.73
	Baseline	CSN/IMPROVE sites	220	1.9	1.3	-0.6	0.9	-34	53	0.06
	Sensitivity	CSN/IMPROVE sites	220	1.9	1.7	-0.2	0.8	-11	42	0.32

Specie	Model Run	Location	N	Observed (ngC/m3)	Predicted (ngC/m3)	Bias (ngC/m3)	Error (ngC/m3)	Fractional Bias (%)	Fractional Error (%)	r
Isoprene SOC	Baseline	Bakersfield	36	96	21	-75	75	-126	128	0.36
		Pasadena	32	42	27	-15	25	-60	83	0.10
Monoterpene SOC	Baseline	Bakersfield	35	56	21	-35	37	-75	89	0.66
		Pasadena	32	82	21	-60	61	-89	93	0.55
Toluene+Xylene SOC	Baseline	Bakersfield	35	59	15	-44	44	-114	114	0.62
		Pasadena	32	125	36	-89	89	-100	100	0.82
Sesquiterpene SOC	Baseline	Bakersfield	41		17					
		Pasadena	41		7					
Benzene SOC	Baseline	Bakersfield	41		2					
		Pasadena	41		2					
Alkane SOC	Baseline	Bakersfield	41		12					
		Pasadena	41		22					
Cloud SOC	Baseline	Bakersfield	41		1					
		Pasadena	41		5					
Naphthalene SOC	Baseline	Bakersfield	36	43						
		Pasadena	32	114						

Specie	Model Run	Location	N	Observed (ppbC)	Predicted (ppbC)	Bias (ppbC)	Error (ppbC)	Fractional Bias (%)	Fractional Error (%)	r
Isoprene VOC 3-hr	Baseline	Bakersfield	5	0.1	0.3	0.2	0.2	79	79	0.79
		Pasadena	8	0.6	0.5	-0.2	0.5	0	84	-0.21
Monoterpene VOC 3-hr	Baseline	Bakersfield	37	1.4	0.5	-0.9	1.0	-72	89	0.25
		Pasadena	28	1.8	0.3	-1.5	1.6	-129	137	0.15
Toluene VOC 3-hr	Baseline	Bakersfield	41	4.3	2.7	-1.6	1.9	-48	55	0.44
		Pasadena	29	7.3	7.7	0.4	3.5	17	44	0.24
Xylene VOC 3-hr	Baseline	Bakersfield	41	4.3	1.8	-2.5	2.5	-82	83	0.34
		Pasadena	29	6.7	4.5	-2.1	2.6	-33	41	0.20
Benzene VOC 3-hr	Baseline	Bakersfield	41	1.2	1.3	0.2	0.5	6	38	0.14
		Pasadena	29	1.5	1.6	0.1	0.5	0	30	0.16
Total VOC 3-hr	Baseline	Bakersfield	41	186.9	63.7	-123.2	124.2	-95	97	0.37
		Pasadena	29	188.9	88.7	-100.1	100.1	-66	66	0.26
Isoprene VOC 1-hr	Baseline	Bakersfield	712	0.4	0.4	0.0	0.3	-21	83	0.15
		Pasadena	718	1.6	0.8	-0.9	1.7	-32	139	-0.10
Monoterpene VOC 1-hr	Baseline	Bakersfield	605	0.8	0.3	-0.6	0.7	-63	101	0.25
		Pasadena	707	0.7	0.2	-0.5	0.5	-105	111	0.05
Toluene VOC 1-hr	Baseline	Bakersfield	737	2.5	1.7	-0.8	1.5	-25	56	0.31
		Pasadena	717	4.0	6.1	2.0	2.8	36	54	0.23
Xylene VOC 1-hr	Baseline	Bakersfield	737	1.9	1.1	-0.7	1.2	-37	64	0.32
		Pasadena	718	3.2	3.4	0.2	1.7	2	51	0.15

Figure 1. Gas (right panel), semi-volatile (middle panel), and particle phase (left panel) CMAQ organic carbon shown by saturation vapor pressure and O:C ratio. Compounds shown in blue exist in the aqueous phase, brown suggest generally fossil in origin, green generally contemporary in origin, and gray both contemporary and fossil in origin. Other known processes such as fragmentation are not shown as they are not currently represented in the modeling system.

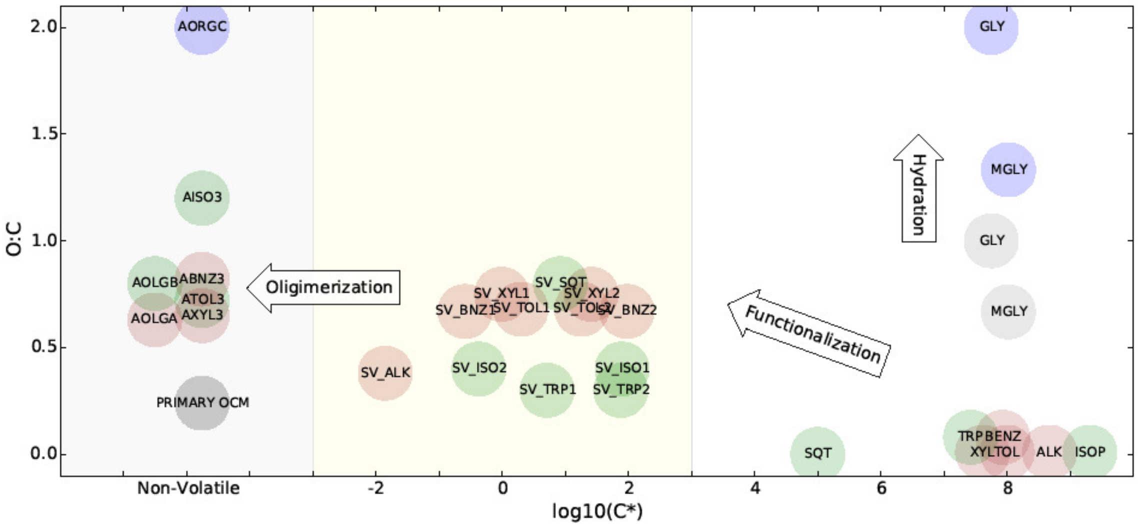

Figure 2. Observed daily 23-h average PM2.5 elemental carbon, PM2.5 contemporary-origin organic carbon, and PM2.5 fossil-origin organic carbon at Pasadena and Bakersfield.

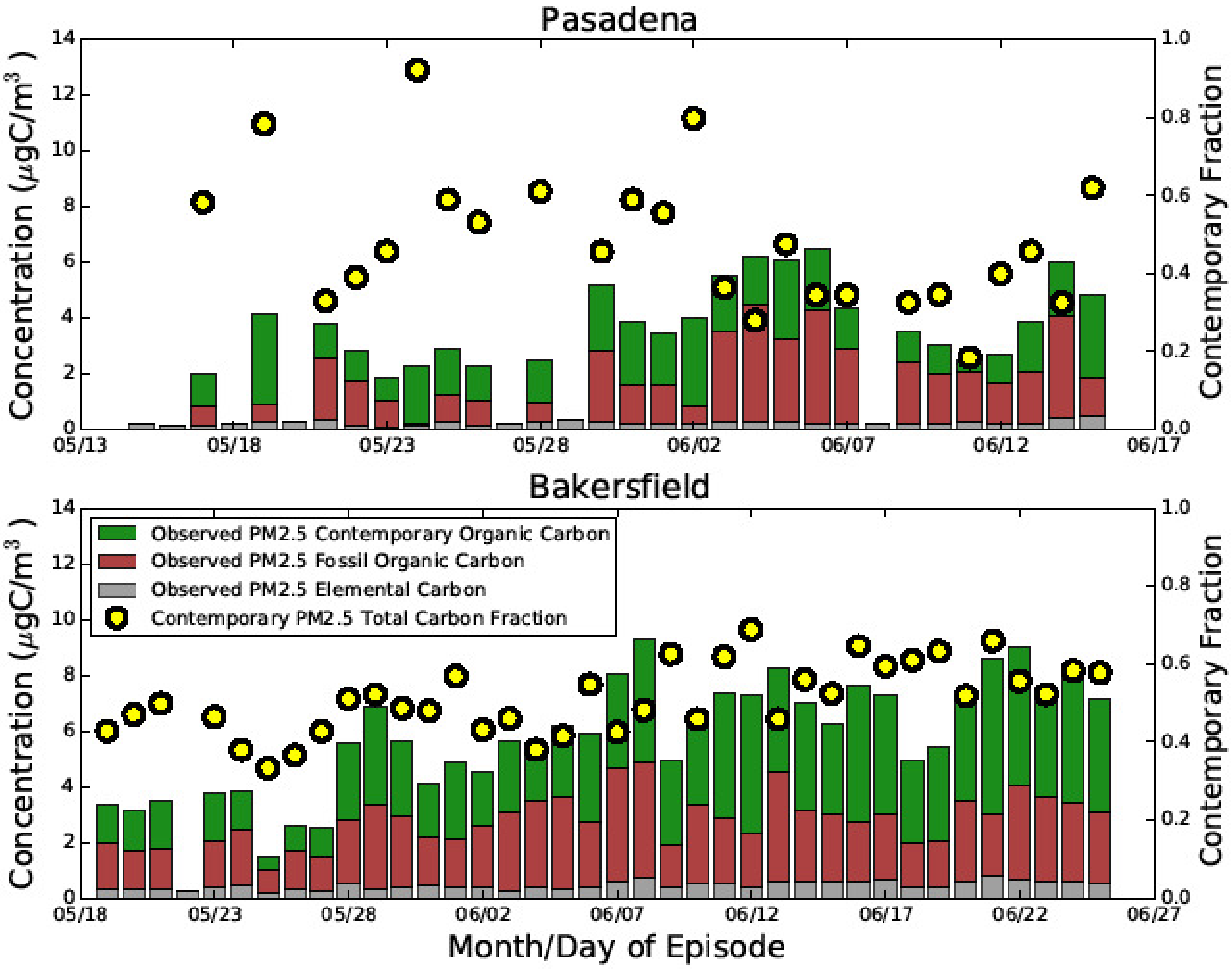

Figure 3. Model predicted and measured $PM_{2.5}$ organic carbon at Pasadena and Bakersfield. The nearby CSN measurements are intended to provide additional context and are not co-located with CalNex measurements or model estimates.

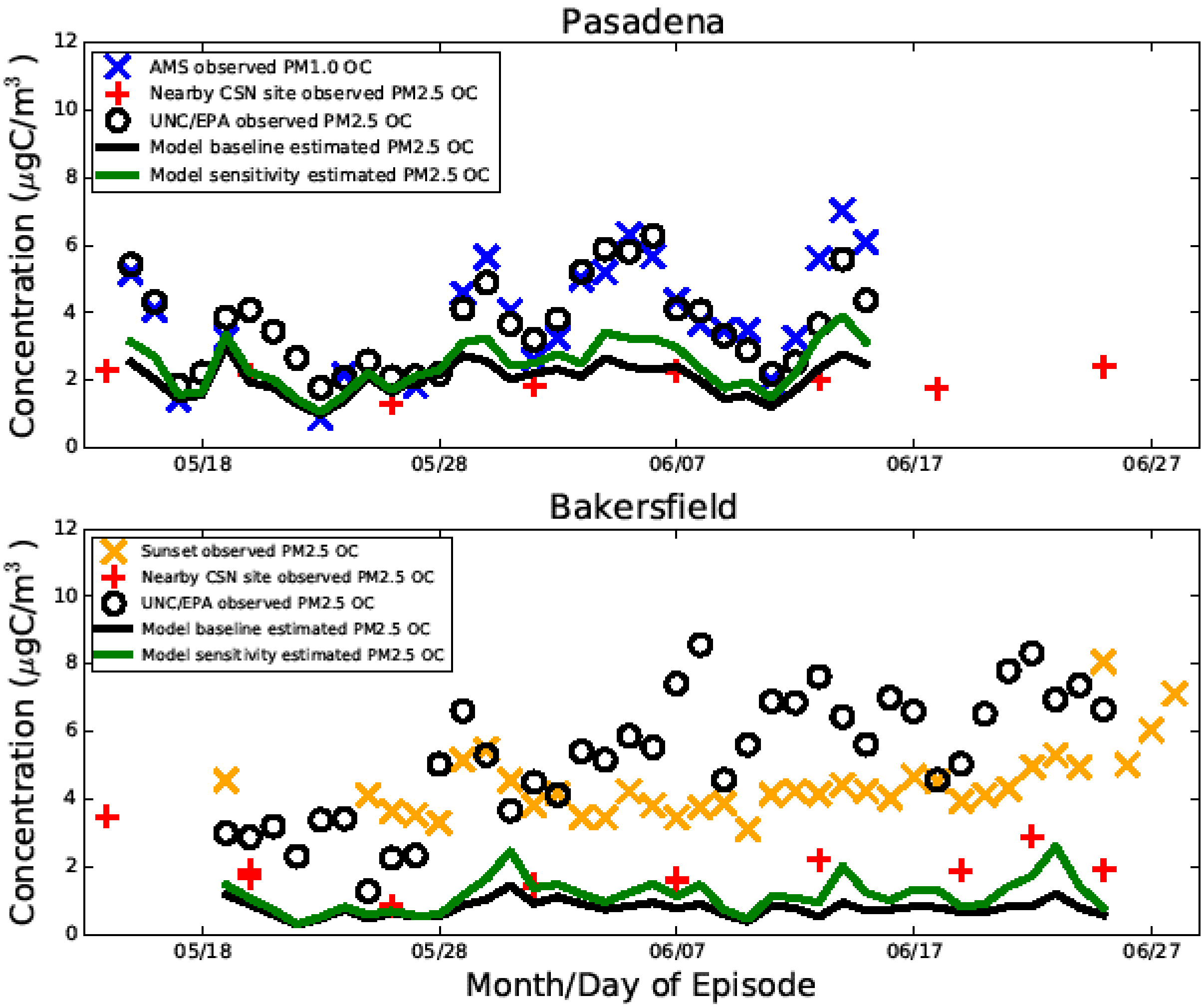

Figure 4. Observed (top row) and modeled (middle and bottom rows) PM2.5 organic carbon at Pasadena and Bakersfield. Mass explained by SOA tracers shown in green (contemporary origin tracers) and brown (fossil origin tracers). Top row gray shading indicates mass not explained by known observed SOC tracers. Middle and bottom row gray shading shows modeled primarily emitted PM2.5 that is both contemporary and fossil in origin. Middle row shows baseline model estimates and bottom row model sensitivity results with increased SOA yields.

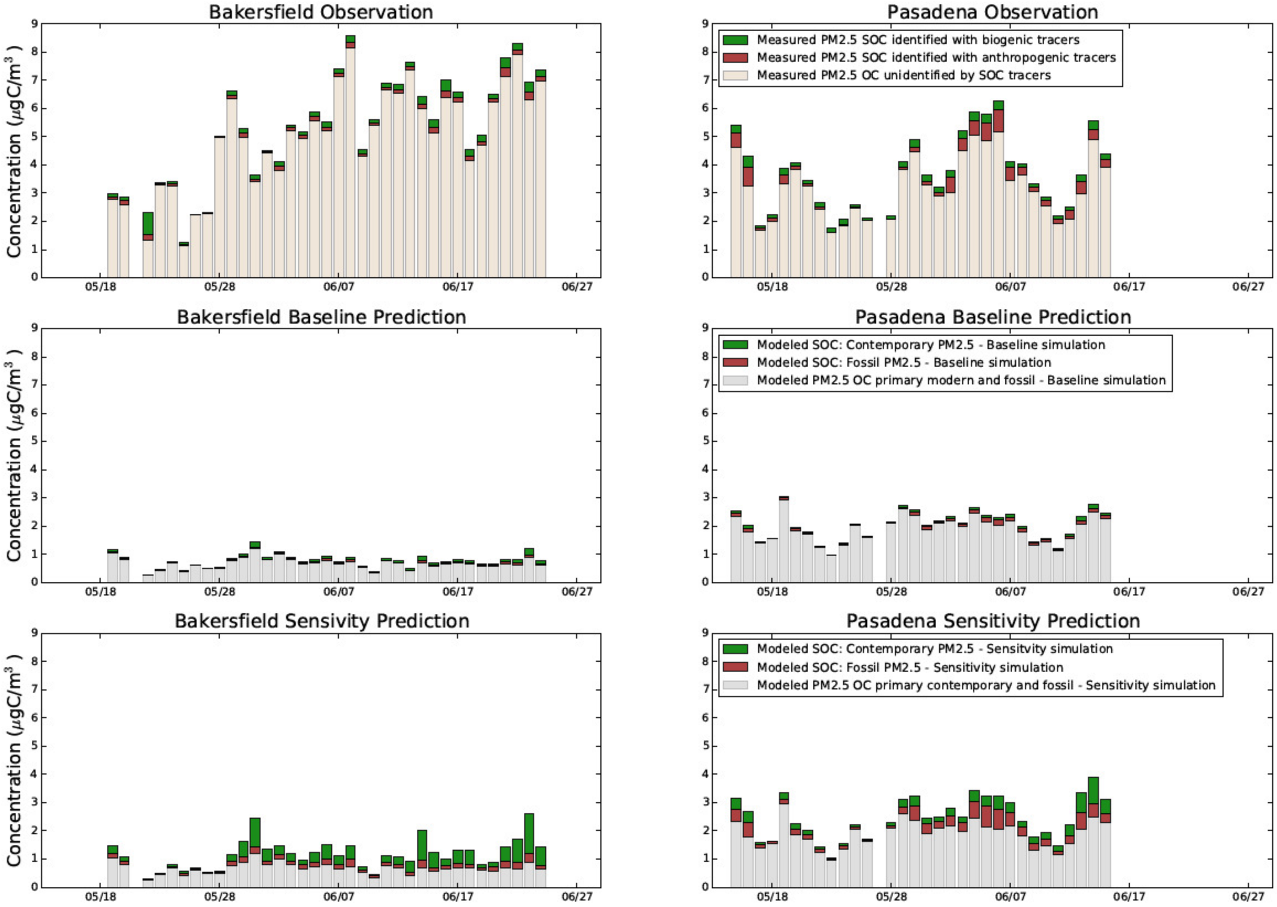

Figure 5. Comparison of CMAQ-predicted and measured VOC (daily average of hourly samples) and corresponding SOC species (daily 23-hr average samples) for Pasadena. Comparison points outside the gray lines indicate model predictions are greater than a factor of 2 different from the measurements.

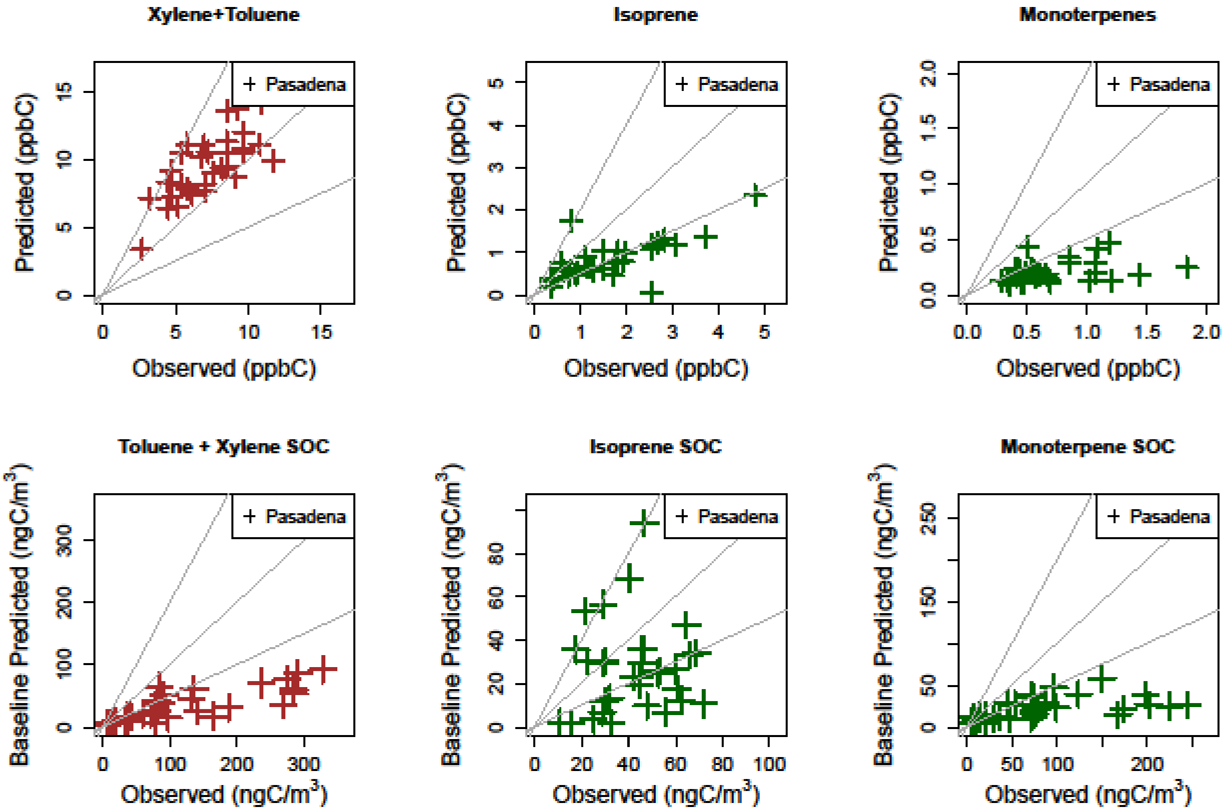

Figure 6. Comparison of CMAQ-predicted and measured VOC (daily average of hourly samples) and corresponding SOC species (daily 23-hr average samples) for Bakersfield. Comparison points outside the gray lines indicate model predictions are greater than a factor of 2 different from the measurements.

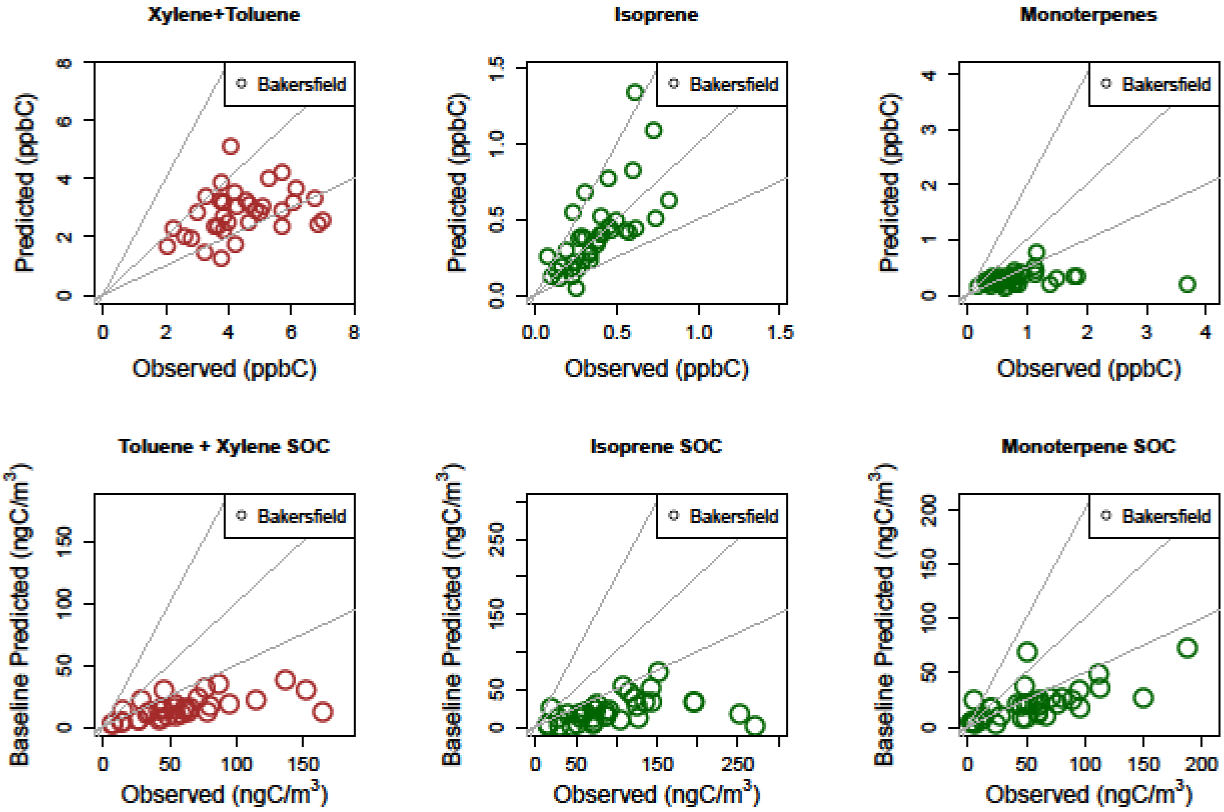

Figure 7. Measured and model estimated OH radical (top) and HO_2+RO_2 (bottom) at Pasadena. The ratio shown on the scatterplots is the episode average model estimate divided by the episode average measured values.

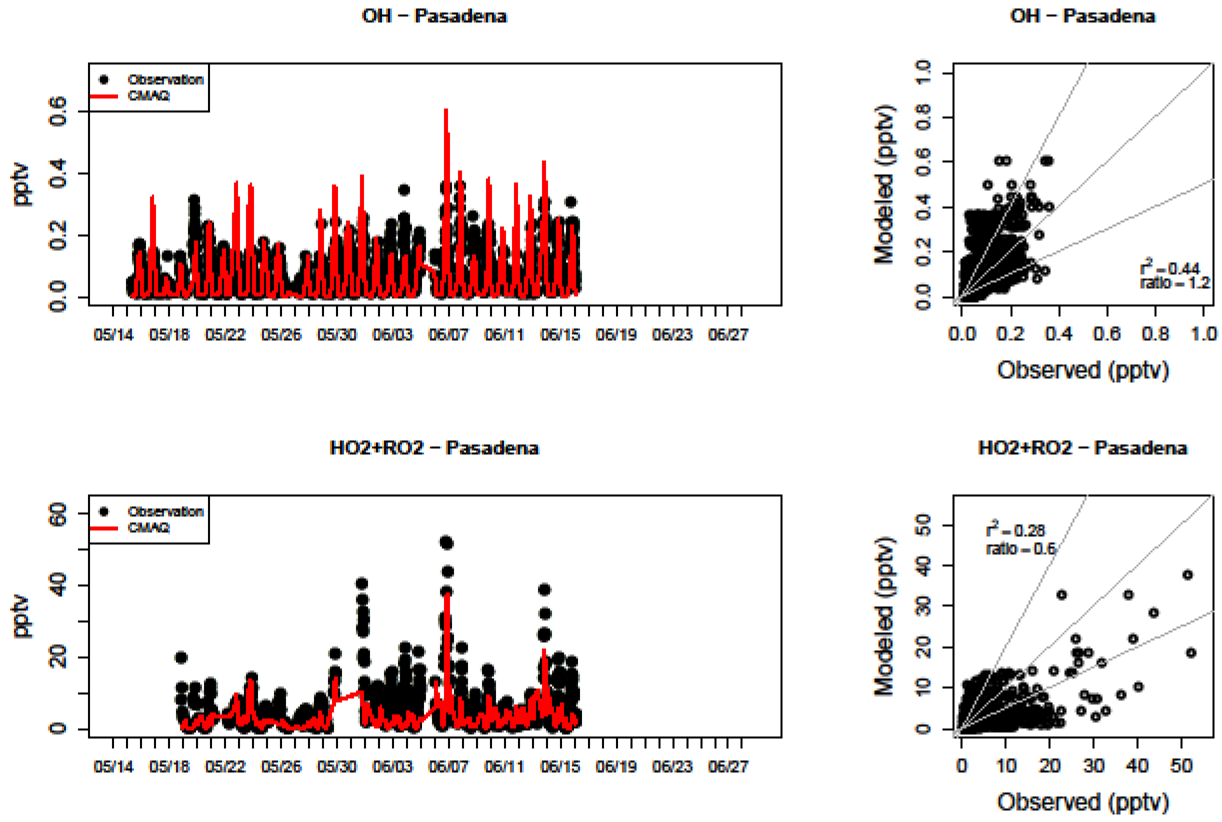

Figure 8. Episode average modeled PM2.5 organic carbon and measurements from both CalNex locations and routine networks including CSN (circles) and IMPROVE (squares). Left panel shows baseline model predictions and right panel shows model estimates with increased SOA yields.